



OPEN ACCESS

EDITED BY

Elisabeth Engel,
Institute for Bioengineering of Catalonia
(IBEC), Spain

REVIEWED BY

Dorsa Dehghan-Baniani,
The Chinese University of Hong Kong,
China
Christopher Synatschke,
Max Planck Institute for Polymer
Research, Germany

*CORRESPONDENCE

Sebastián L. Vega,
vegas@rowan.edu

SPECIALTY SECTION

This article was submitted to
Biomaterials Science for Regenerative
Therapies,
a section of the journal
Frontiers in Biomaterials Science

RECEIVED 19 May 2022

ACCEPTED 30 June 2022

PUBLISHED 22 July 2022

CITATION

Gultian KA, Gandhi R, DeCesari K,
Romiyo V, Kleinbart EP, Martin K,
Gentile PM, Kim TWB and Vega SL
(2022), Injectable hydrogel with
immobilized BMP-2 mimetic peptide for
local bone regeneration.
Front. Front. Biomater. Sci. 1:948493.
doi: 10.3389/fbiom.2022.948493

COPYRIGHT

© 2022 Gultian, Gandhi, DeCesari,
Romiyo, Kleinbart, Martin, Gentile, Kim
and Vega. This is an open-access article
distributed under the terms of the
[Creative Commons Attribution License
\(CC BY\)](#). The use, distribution or
reproduction in other forums is
permitted, provided the original
author(s) and the copyright owner(s) are
credited and that the original
publication in this journal is cited, in
accordance with accepted academic
practice. No use, distribution or
reproduction is permitted which does
not comply with these terms.

Injectable hydrogel with immobilized BMP-2 mimetic peptide for local bone regeneration

Kirstene A. Gultian¹, Roshni Gandhi¹, Kayla DeCesari¹,
Vineeth Romiyo², Emily P. Kleinbart², Kelsey Martin²,
Pietro M. Gentile², Tae Won B. Kim^{1,2} and Sebastián L. Vega^{1*}

¹Department of Biomedical Engineering, Rowan University, Glassboro, NJ, United States, ²Department of Orthopaedic Surgery, Cooper University Health Care, Camden, NJ, United States

Osteoporosis is a disease characterized by a decrease in bone mineral density, thereby increasing the risk of sustaining a fragility fracture. Most medical therapies are systemic and do not restore bone in areas of need, leading to undesirable side effects. Injectable hydrogels can locally deliver therapeutics with spatial precision, and this study reports the development of an injectable hydrogel containing a peptide mimic of bone morphogenetic protein-2 (BMP-2). To create injectable hydrogels, hyaluronic acid was modified with norbornene (HANor) or tetrazine (HATet) which upon mixing click into covalently crosslinked Nor-Tet hydrogels. By modifying HANor macromers with methacrylates (Me), thiolated BMP-2 mimetic peptides were immobilized to HANor via a Michael addition reaction, and coupling was confirmed with ¹H NMR spectroscopy. BMP-2 peptides presented in soluble and immobilized form increased alkaline phosphatase (ALP) expression in MSCs cultured on 2D and encapsulated in 3D Nor-Tet hydrogels. Injection of bioactive Nor-Tet hydrogels into hollow intramedullary canals of Lewis rat femurs showed a local increase in trabecular bone density as determined by micro-CT imaging. The presented work shows that injectable hydrogels with immobilized BMP-2 peptides are a promising biomaterial for the local regeneration of bone tissue and for the potential local treatment of osteoporosis.

KEYWORDS

osteoporosis, injectable hydrogels, hyaluronic acid, BMP-2, DWIVA peptides, bone regeneration

1 Introduction

Osteoporosis is characterized by a reduction in bone mineral density and disruption of bone microarchitecture (Wright et al., 2014). Osteoporosis is the most common chronic metabolic bone disease with an estimated 200 million people affected worldwide (Sozen et al., 2017). According to the International Osteoporosis Foundation, 1 in 3 women above the age of 50 and 1 in every 5 men will experience fragility fractures resulting from osteoporosis in their lifetime (Cooper, 1999). Osteoporosis increases the

chances of fragility fractures after a low-level fall, with a mortality rate of up to 69% within 10 years (Rachner et al., 2011). Risk factors for osteoporosis include genetics, being of postmenopausal age, substance abuse, poor dietary intake, and inactivity (Van der Voort et al., 2001). These risk factors disrupt bone remodeling, a dynamic physiological process in which bone tissue is resorbed by osteoclasts and formed by osteoblasts (Corral et al., 1998; Sozen et al., 2017). In osteoporosis, the rate of bone resorption is greater than the rate of bone formation, especially in major weight-bearing bones including vertebrae in the lumbar spine and femurs (Deligianni et al., 1991; Sozen et al., 2017). In the early stages of osteoporosis, bone loss is mainly observed in trabecular or cancellous bone, made up of a trabeculae network with high bone turnover (Li and Aspden, 1997; Zebaze et al., 2010; Osterhoff et al., 2016). Current treatments for osteoporosis are antiresorptive and anabolic drugs which can cause systemic side effects including oncogenesis (Sozen et al., 2017; Tu et al., 2018). Hormonal therapies (e.g., estrogen supplementation) are used as a last resort and only prescribed to high-risk post-menopausal women because it can cause adverse side effects including blood clots (Sozen et al., 2017).

Efforts to develop alternative strategies to regenerate bone have utilized recombinant human bone morphogenetic protein 2 (BMP-2), a potent inducer of osteogenesis *in vivo* (Murakami et al., 2003; Takahashi et al., 2005; Tsuji et al., 2006; Kwong et al., 2009; Mehta et al., 2012). The osteogenic signaling cascade begins when BMP-2 binds to BMP-receptor type II, which leads to the phosphorylation (activation) of BMP-receptor type I, and ultimately to the phosphorylation of Smad1, a cytoplasmic signaling molecule for BMP-2. Phosphorylated Smad1 then localizes to the nucleus and controls gene expression to initiate osteogenic differentiation (Wrana, 2000; Ito and Miyazono, 2003; Waite and Eng, 2003). *In vitro*, embryonic stem cells, human mesenchymal stem cells (MSCs), and C2C12 myoblasts exposed to BMP-2 express increased levels of cytoplasmic ALP, a well-established biomarker of osteogenesis (Zhao et al., 2006; Park et al., 2010). Despite its osteoinductive properties, the clinical use of BMP-2 is limited by unwanted side effects. For instance, collagen scaffolds with high doses of untethered BMP-2 used for spinal fusions have resulted in serious complications including ectopic bone formation and impaired neurological function (Shields et al., 2006; Garrison et al., 2007; Wong et al., 2008).

BMP-2 is a large and expensive growth factor, and BMP-2 based therapies are associated with inconsistent outcomes and safety concerns. Peptides that mimic the bioactivity of native BMP-2 are an inexpensive and potentially more efficacious substitute that can be incorporated into biomaterials. Specifically, the DWIVA peptide sequence from BMP-2 has high receptor-binding activity and specificity to BMP-receptor types I and II (Lee et al., 2009), and several groups have explored the use of this sequence to enhance osteogenic differentiation and

bone formation (Seol et al., 2006; Lee et al., 2009; Madl et al., 2014). Seol et al. (2006) found that osteoblast-like MC3T3-E1 cells cultured on titanium (Ti) chemically modified with DWIVA peptides had higher levels of ALP, and DWIVA-treated Ti dental implants induced increased bone formation *in vivo*. MSCs encapsulated in DWIVA-functionalized self-assembling nanofibrous hydrogel networks and alginate hydrogels also commit to osteogenic lineages, as evidenced by increased ALP activity and mineralization (Lee et al., 2009; Madl et al., 2014).

Hyaluronic acid (HA) is an abundant extracellular matrix component that mediates cellular signaling, matrix organization, and morphogenesis (Toole, 2001, 2004). HA polymers are amenable to chemical modifications through carboxyl and hydroxyl functional groups that can be used as macromers to create highly tunable hydrogels via various polymerization schemes (Burdick and Prestwich, 2011; Highley et al., 2016). For instance, Diels-Alder reactions between macromers modified with dienes (e.g., Nor) and dienophiles (e.g., Tet) yield self-forming hydrogels that can be injected (Alge et al., 2013; Desai et al., 2015). In this study, we hypothesize that HA modified with Nor or Tet moieties can be used to create injectable DWIVA-functionalized Nor-Tet hydrogels that enhance osteogenic differentiation of MSCs *in vitro* and induce trabecular bone growth *in vivo*. To test this hypothesis, we developed an injectable HA hydrogel system by modifying HA with Nor (HANor) or Tet (HATet) moieties. BMP-2 signals were immobilized in the hydrogels by methacrylating HANor macromers (HANorMe) and pre-coupling Me-groups with thiolated DWIVA peptides via an aqueous Michael addition reaction. Osteogenic differentiation of MSCs cultured atop or within DWIVA-functionalized hydrogels were investigated by quantifying ALP *via* fluorescent imaging-based analysis. New trabecular bone formation in rat femurs injected with HA Nor-Tet hydrogels with or without DWIVA peptide was also evaluated using micro-computed tomography (micro-CT).

2 Materials and methods

2.1 Materials

Sodium hyaluronate (NaHA, 60 kDa, HA60K-5) was purchased from Lifecore Biomedical (Chaska, MN). Dowex® resin 50WX8 hydrogen form, 100–200 mesh, methacrylic anhydride (MA), triethanolamine (TEOA), and Fast Blue RR Assay (fast blue) were purchased from Sigma Aldrich (Burlington, MA). Dimethyl sulfoxide (DMSO), benzotriazole-1-yl-oxy-tris-(dimethylamino)-phosphonium hexafluorophosphate (BOP), β -(N-morpholino)ethanesulfonic acid (MES), and SpectraPor 6–8 kDa molecular weight cutoff dialysis tubing were purchased from Millipore Sigma (St. Louis, MO). Tetrabutylammonium hydroxide (TBA-OH) was purchased

from Acros Organics (Geel, Belgium). 5-norbornene-2-methylamine (Nor-NH₂) and N-hydroxysuccinimide (NHS) were purchased from TCI America (Portland, OR). 1-(3-dimethylaminopropyl)-3-ethylcarbodiimide (EDC) and Hoechst were purchased from Thermo Scientific (Waltham, MA). Tetrazine-amine (Tet-NH₂) was purchased from Kerafast (Boston, MA). Thiol-containing peptide mimic of BMP-2 with sequence GCGGGDWIVAG (DWIVA) was purchased from GenScript (Piscataway, NJ). Human MSCs from bone marrow and Osteogenic Differentiation BulletKit™ Medium (OS Medium) were purchased from Lonza (Walkersville, MD). Minimum essential medium alpha (MEM-α) with no nucleosides, penicillin/streptomycin (10,000 U/ml), and fetal bovine serum (FBS) were purchased from Gibco (Waltham, MA). Silicone elastomer, Sylgard™ 184 was purchased from Electron Microscopy Sciences (Hatfield, PA). Isoflurane solution and 70% isopropyl alcohol were purchased from Covetrus (Portland, ME). Buprenorphine SR 1 mg/ml and meloxicam SR 2 mg/ml were purchased from ZooPharm (Laramie, WY). 2% chlorohexidine was purchased through Covetrus (Portland, ME) and supplied by Vedco (Saint Joseph, MO).

2.2 Hydrogel macromer synthesis and characterization

2.2.1 HANor

Carboxyl groups in HA were modified with Nor as previously described (Vega et al., 2018). Briefly, NaHA was converted to its tetrabutylammonium salt (HATBA) by dissolving in distilled water (2% w/v) and mixing with Dowex resin (3 g resin per 1 g NaHA) for two hours at room temperature. The resin was then vacuum filtered, and the pH was adjusted to 7.02 using TBA-OH diluted in water (1:1 v/v). The resulting HATBA solution was frozen and lyophilized. Carboxyl groups in HATBA were then modified with Nor via amidation with Nor-NH₂ (0.4 mmol per 1 g of HATBA) in anhydrous DMSO (0.5 ml per 0.1 g HATBA) and BOP (0.38 g per 1 g HATBA) under nitrogen for two hours at room temperature. The reaction was quenched with cold distilled water, dialyzed with SpectraPor dialysis tubing, frozen, and lyophilized. The synthesized HANor macromer had ~50% of its repeat units functionalized with Nor, as analyzed with 1H NMR spectroscopy. The percentage of modification was calculated by comparing the integral of the methyl HA peaks between δ 1.8–2.0 ppm to the vinyl proton peaks of Nor between δ 6.2–6.3 ppm (Miao et al., 2015).

2.2.2 HATet

Carboxyl groups in HA were modified with Tet using a modified procedure previously described (Desai et al., 2015). Briefly, HATBA was dissolved (1% w/v) in 100 mM MES buffer (pH 6). EDC, NHS, and Tet-NH₂ were added at a 1:4:1 M ratio at

0.5 mmol Tet per g of HATBA and reacted overnight at room temperature. The HATet solution was then dialyzed with SpectraPor dialysis tubing, frozen, and lyophilized. 1H NMR spectroscopy analysis confirmed that ~40% of HATet repeat units were functionalized with Tet. The percentage of modification was calculated by comparing the integral of the methyl HA peaks between δ 1.8–2.0 ppm to the carboxyl proton peak of tetrazine between δ 10.0 and 10.5 ppm and aromatic proton peak of tetrazine between δ 7.0 and 8.5 ppm (Koshy et al., 2016).

2.2.3 HANorDWIVA

Hydroxyl groups in HANor were first modified with Me to form HANorMe via esterification with MA by adapting a previously described protocol (Smeds and Grinstaff, 2000). HANor was dissolved (1% w/v) in distilled water at 4°C. A 15-fold molar excess of MA was added dropwise while maintaining pH between 8.5 and 9.0. After all MA was added, the solution was left stirring overnight at room temperature. The HANorMe solution was then dialyzed with SpectraPor dialysis tubing, frozen, and lyophilized. 1H NMR spectroscopy analysis confirmed that ~60% of HANorMe repeat units were functionalized with Me. The percentage of modification was calculated by comparing the integral of the HA peaks between δ 1.8–2.0 ppm to the alkene proton peaks of Me between δ 5.5–6.5 ppm (Yousefi et al., 2018).

To peptide-functionalize HANorMe, thiols in cysteine-containing peptides were coupled to Me groups in HANorMe via an aqueous Michael addition reaction (Li et al., 2010). Briefly, HANorMe was dissolved (1% w/v) in 200 mM TEOA buffer (pH 8) at room temperature. Thiolated DWIVA (sequence: GCGGGDWIVAG) in solution (50 mM in PBS) was added dropwise to reach a final DWIVA concentration that corresponds to an effective concentration of either 0.50 mM or 2 mM for 2% w/v HA Nor-Tet hydrogels (Supplementary Table S1) (Lee et al., 2009; Madl et al., 2014). The HANorDWIVA solution was then dialyzed with SpectraPor dialysis tubing, frozen, and lyophilized. 1H NMR spectroscopy analysis confirmed that 5% (for 0.5 mM) and 16% (for 2 mM) of Me groups were coupled with DWIVA. The percentage of Me-DWIVA coupling was calculated by comparing the integral of alkene proton peaks of Me between δ 5.5–6.5 ppm (Yousefi et al., 2018) to the protons in the amino group of cysteine moiety between δ 0.50–1.50 ppm (Madl et al., 2014).

2.3 Characterization of Nor-Tet hydrogels

To characterize the hydrogels, rheology and compression mechanical testing were performed. Rheological properties of Nor-Tet hydrogels were measured using a Discovery Hybrid Rheometer (DHR-3, TA Instruments, New Castle, DE) with a 20 mm diameter 1° cone upper plate geometry and a lower plate

temperature of 37°C. Samples were prepared by dissolving HANor (with or without DWIVA functionalization) and HATet separately in PBS, followed by mixing at a 1:1 stoichiometric ratio, resulting in a final macromer concentration of 2% w/v. Immediately after mixing, 40 µl of the solution was pipetted to the center of the rheometer stage and the shear storage (G') and loss (G'') moduli were monitored. To measure plateau G' and gelation kinetics, time sweeps were performed for 1 h at 1 Hz and 1% oscillatory strain. Bulk mechanical properties of 2% w/v self-forming hydrogels were measured using an EZ-SX Mechanical Tester (Shimadzu, Long Beach, CA) equipped with a 50 N compression load. Briefly, hydrated HANor or HANorDWIVA and HATet were mixed and pipetted into cylindrical polydimethylsiloxane (PDMS) molds (2 mm height, 8 mm diameter). The hydrogels were allowed to form for 30 min before incubating in PBS overnight at 37°C. Formed cylindrical Nor-Tet hydrogels were compressed until 30% strain, and the elastic modulus (E) was determined using the slope of the stress-strain curve between 10% and 20% strain.

2.4 Cell culture

Human primary MSCs were cultured in 100 mm petri dishes in Growth Medium (MEM- α supplemented with 10% FBS and 1% P/S). To study the effects of soluble DWIVA on stem cell cultures, MSCs were seeded on top of glass coverslips (12 mm diameter) at a density of 3,000 cells per cm². After 6 h in culture, media was replaced with either Growth Medium (0 mM DWIVA), Growth Medium supplemented with low (0.50 mM) or high (2.0 mM) DWIVA, or OS Medium.

To study the effects of tethered DWIVA on 2D hydrogel cultures, 2% w/v HA Nor-Tet hydrogels with varying degrees of DWIVA functionalization (0, 0.5, 2 mM) were formed on PDMS molds (11 mm diameter, 1 mm height) for 30 min followed by incubation in Growth Medium for 30 min at 37°C. MSCs were seeded on top of these hydrogels at a density of 3,000 cells per cm². To study the effects of DWIVA in 3D hydrogel cultures, MSC-laden (2×10^6 cells/ml) 2% w/v Nor-Tet hydrogels with varying degrees of DWIVA functionalization (0, 0.5, 2 mM) were formed on PDMS molds (8 mm diameter, 2 mm height) for 2 min followed by incubation in Growth Medium for 30 min at 37°C. Appropriate media were replenished every 48 h and all experiments were cultured for 7 days.

2.5 Staining and imaging-based analysis

After 7 days in culture, samples were fixed with 10% neutral buffered formalin for 10 min (glass, 2D hydrogels) or 30 min (3D hydrogels) at room temperature. To visualize cellular ALP, fast blue was added for 1 h (glass, 2D hydrogels) or 3 h (3D hydrogels). To visualize individual nuclei, samples were

stained for double stranded DNA with Hoechst (1:1000) for 5 min (glass, 2D hydrogels) or 15 min (3D hydrogels). Acquisition of immunofluorescence images was performed with a Nikon A1 confocal microscope. Images were taken at 20 \times magnification and at laser wavelengths of 405 nm (nuclei) and 640 nm (ALP) (glass, 2D and 3D hydrogels). Image stacks were taken at height of 200 µm with a step size of 3.2 µm (3D hydrogels).

Mean fluorescence intensity (MFI) of cellular ALP was determined using ImageJ software (National Institute of Health, Bethesda, MD, United States). Briefly, nuclei stacks were binarized using the Otsu thresholding method. Binarized nuclei stacks were dilated, and the nuclei stacks were subtracted from the dilated stacks resulting in rings. The rings were converted into masks and overlaid on the ALP channel stacks. The 3D Objects Counter feature was then applied to calculate the surface area of the rings and the Measure function was used to determine the integrated density of the rings. The MFI value of every cell was calculated by dividing its mean grey value by area. The MFI values of Growth Medium and OS Medium groups were processed using a k-means clustering algorithm to determine the boundary between MSCs with low (ALP-negative) and high (ALP-positive) MFI. The selected threshold MFI covers 95% of ALP-negative cells (Vega et al., 2012).

2.6 Animal protocol

The animal experiment was approved by the Cooper University Health Care's Institutional Animal Care and Use Committee (IACUC). Experiments were performed on 8-week-old male Lewis rats (Charles River Laboratories, Raleigh, NC) weighing approximately 275–300 g. The rats were housed in a 12-h dark-light cycle where they had access to food and water *ad libitum*. The rats were randomly divided into three groups: drilled canal alone, injectable hydrogel, and injectable hydrogel with 2 mM DWIVA peptide. The procedures were performed under anesthesia using inhaled isoflurane solution and buprenorphine SR. Once anesthetized, surgical sites were prepared by shaving the ventral aspect of the abdomen and hind legs and scrubbed with 2% chlorhexidine and 70% isopropyl alcohol. A standard median parapatellar approach to bilateral knees was performed. The distal femurs were exposed, and the femoral notch was identified. Utilizing a 1 mm sterile drill, the intramedullary canal was drilled and checked on fluoroscopy for placement. Three passes with the drill were performed to adequately remove native bone marrow and trabecular bone. The femurs were then filled with 0.2 ml of 2% w/v self-forming hydrogel solution via injection using a 25-gauge syringe. Bone wax was placed over the hole after injection. Closure of the arthrotomy and skin was performed with Vicryl sutures. Following closure of the surgical sites, animals were

given meloxicam SR (2 mg/ml) for pain alleviation and subsequently returned to their housing where they were monitored until they recovered from the surgical anesthesia. All rats were euthanized 4 weeks post-injection and the left and right femurs were harvested. The femurs were fixed with 10% neutral-buffered formalin for 24 h, washed with distilled water, and stored in 70% ethanol at 4°C until micro-CT imaging.

2.7 Micro-CT

The distal shaft (midshaft down to the metaphysis) of extracted femurs were scanned using micro-CT (microCT 45, ScancoMedical AG, Brüttsellen, Switzerland) at 10.4 μm isotropic resolution, with 55 kVp energy, and 400 ms integration time. This region was chosen to evaluate the effects of injectable DWIVA hydrogels on trabecular bone formation. At the center of the distal shaft, a 200-slice-thick volume of interest (VOI) was identified, Gaussian filtered (sigma = 1.2, support = 2), and bone was identified by applying a global threshold (220 mg hydroxyapatite per cm³). Manufacturer-provided software for 3D standard microstructural analysis was used to generate 3D axial views of the 200-slice-thick VOIs and coronal views of the 1031-slice-thick distal shaft.

2.8 Statistical analysis

Statistical analysis was performed using GraphPad Prism (version 9.3.1, GraphPad Software, Inc., La Jolla, CA). All experiments were carried out in triplicate and single cell analysis was done with at least 50 cells per group. All graphs represent mean ± standard deviation (SD). Analysis of variance (ANOVA) was performed followed by Tukey's test for post-hoc analysis. Differences among groups are stated as $p < 0.05$ (*), $p < 0.01$ (**), $p < 0.001$ (***), and (ns) when differences between groups are not statistically significant.

3 Results

3.1 Mechanics and gelation kinetics of injectable HA hydrogels are preserved after DWIVA coupling

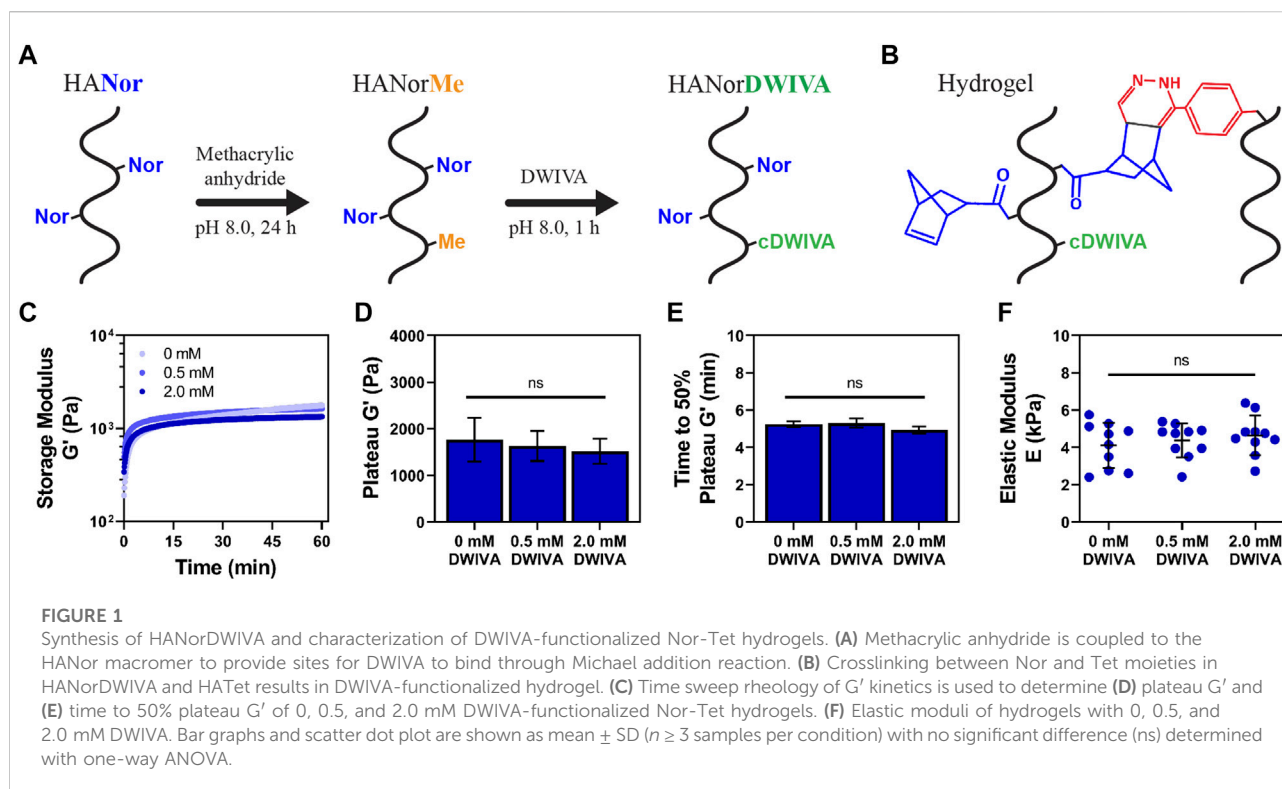
The percentage modification of HANor and HATet with Nor and Tet was determined to be ~50% and ~40% through ¹H-NMR, respectively. Modification of HANor with Me provide sites for coupling thiolated DWIVA peptides to the HANor macromer backbone (Figure 1A). ¹H-NMR shows that HANor has a Me modification of ~80%. Coupling HANorMe with 0.5 and 2.0 mM DWIVA results in 5% and 16% of Me groups bound to peptide,

respectively (Supplementary Figure S1). Mixing of hydrated HANorDWIVA with hydrated HATet results in hydrogel formation through crosslinking between Nor and Tet moieties (Figure 1B). Material characterization of Nor-Tet hydrogels functionalized with 0, 0.5, or 2.0 mM DWIVA shows that mechanics and gelation time are not affected by the DWIVA peptide. Additionally, DWIVA functionalization does not affect the equilibrium swelling ratio of HA Nor-Tet hydrogels (Supplementary Table S2). Frequency sweep rheology (0.1–10 Hz) at 37°C shows constant storage modulus (G') at every time point for Nor-Tet hydrogels with 0, 0.5, and 2.0 mM DWIVA, respectively (Figure 1C). Time sweep rheology (1 Hz) at 37°C shows that plateau G' values are $1,767 \pm 468$, $1,630 \pm 323$ Pa, and $1,517 \pm 268$ Pa for Nor-Tet hydrogels with 0, 0.5, and 2.0 mM DWIVA, respectively (Figure 1D). The time to 50% plateau G' values are 5.25 ± 0.16 min, 5.30 ± 0.24 min, and 4.93 ± 0.20 min for Nor-Tet hydrogels with 0, 0.5, and 2.0 mM DWIVA, respectively (Figure 1E). Compression testing shows elastic moduli (E) values of 4.12 ± 1.22 kPa, 4.38 ± 0.92 kPa, and 4.64 ± 1.07 kPa for Nor-Tet hydrogels with 0, 0.5, and 2.0 mM DWIVA, respectively (Figure 1F).

3.2 Soluble and immobilized DWIVA enhance ALP levels of MSCs on 2D cultures

MSCs seeded on glass cultured in Growth Medium supplemented with 2.0 mM DWIVA show significantly more positive staining for ALP (dark blue) compared to cells cultured in Growth Medium or in Growth Medium supplemented with a lower (0.50 mM) DWIVA concentration (Figure 2A). Confocal images of MSC cultures stained for ALP (magenta) and nuclei (blue) show a progressive increase in ALP signal with increasing DWIVA concentration (Figure 2B). To distinguish between ALP(+) and ALP(−) MSCs, the mean fluorescence intensity (MFI) of intracellular ALP was first determined for individual MSCs using imaging-based analysis with ImageJ (Supplementary Figure S2). The MFI values of the Growth Medium and OS Medium groups were processed using a k-means clustering algorithm to determine the boundary between ALP(−) and ALP(+) clusters, resulting in an MFI cutoff value of 52, which covers 95% of ALP(−) MSCs (Figure 2C). The MFI threshold value is used as a filter that assigns MSCs as ALP(−) (MFI < 52) or ALP(+) (MFI ≥ 52) (Figure 2D). Using this technique, the percentage of ALP(+) MSCs on glass is $7.5\% \pm 2.1\%$ (Growth Medium), $14.1\% \pm 4.3\%$ (0.5 mM DWIVA), $67.5\% \pm 3.7\%$ (2.0 mM DWIVA), and $92.1\% \pm 3.9\%$ (OS Medium) (Figure 2E).

HANorMe was pre-functionalized with thiolated RGD (2 mM) and with 0, 0.5, or 2 mM thiolated DWIVA. Pre-functionalized HANorMe macromers were then mixed with HATet to form Nor-Tet hydrogels that were seeded with MSCs (Figure 3A). Representative MSCs (ALP, magenta;



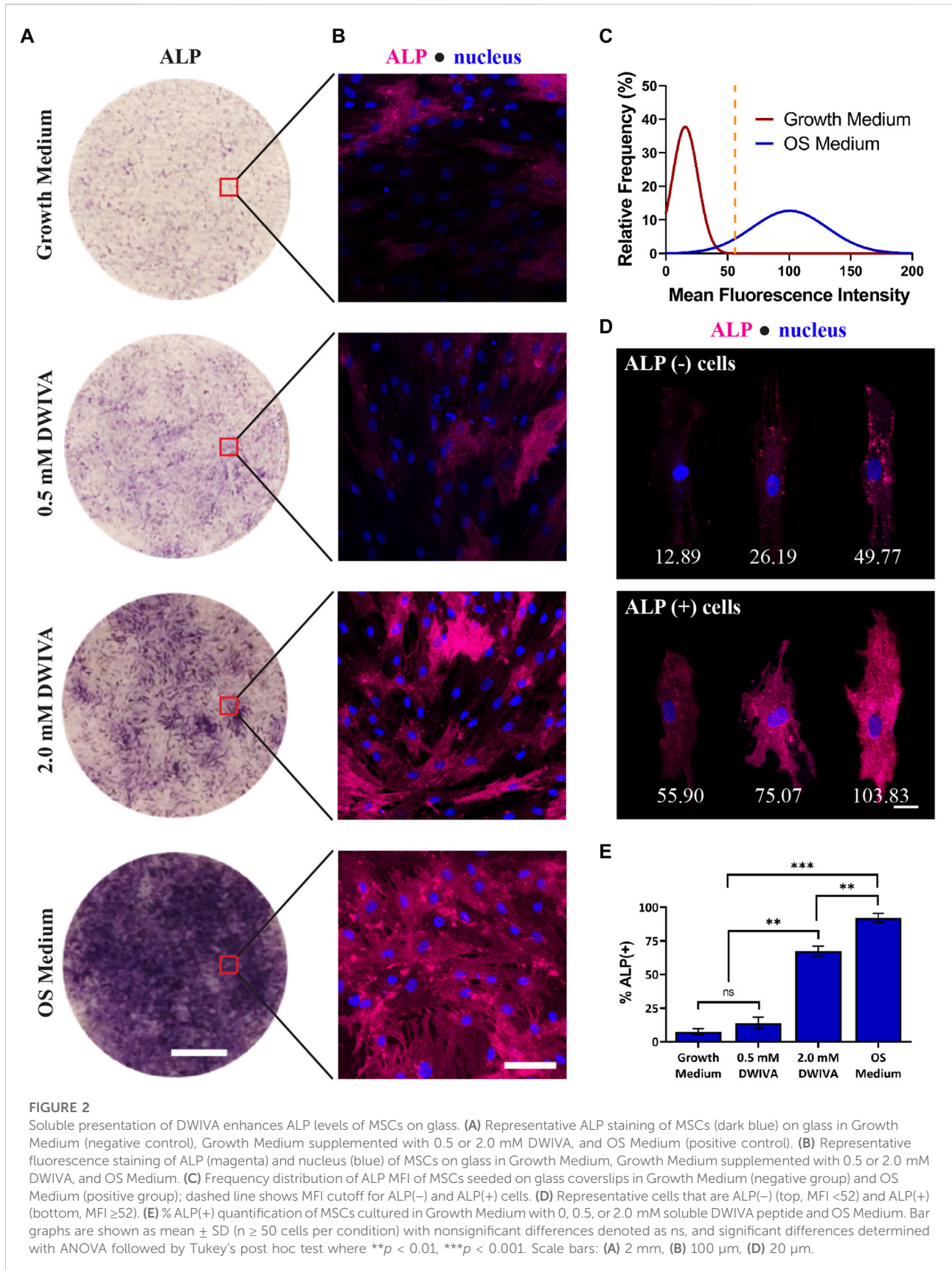
nuclei, blue) in different treatment groups show more magenta signal in cells atop 2D hydrogels coupled with 2.0 mM DWIVA compared to cells atop hydrogels with lower DWIVA (0, 0.5 mM) concentrations (Figure 3B). A k-means clustering algorithm was applied for MFI values of MSCs on Growth Medium (negative group) and OS Medium (positive group) to determine an MFI cutoff of 50, which covers 95% of ALP(−) MSCs (Figure 3C). The percentage of ALP(+) MSCs on Nor-Tet hydrogels is 12.1% \pm 4.5% (0 mM DWIVA), 19.3% \pm 4.5% (0.5 mM DWIVA), 42.9% \pm 3.8% (2.0 mM DWIVA), and 74.1% \pm 4.1% (OS Medium) (Figure 3D).

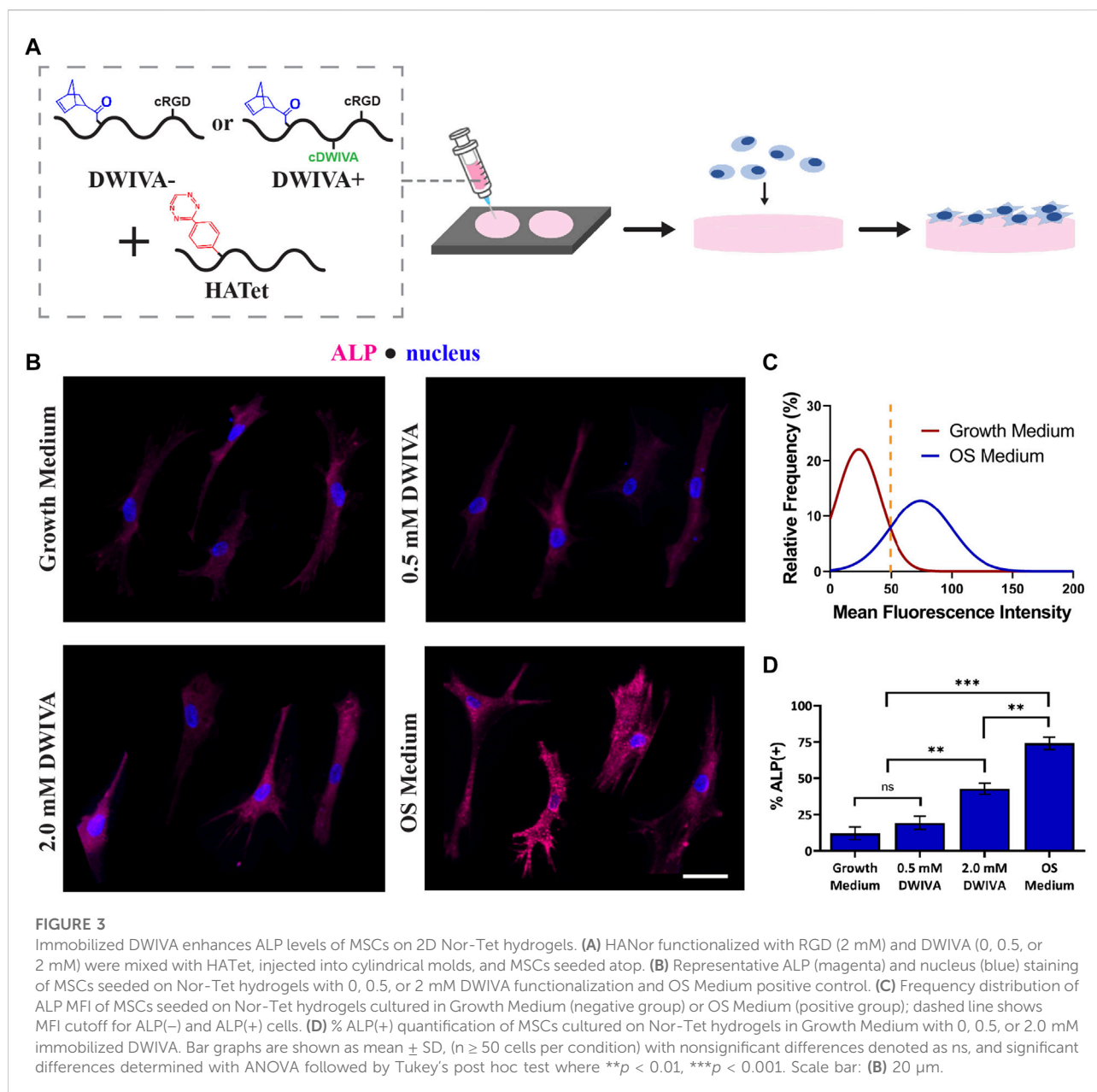
3.3 Injectable DWIVA-functionalized Nor-Tet hydrogels enhance ALP levels of encapsulated MSCs and induce trabecular bone growth

MSCs were mixed in HATet and HANor pre-functionalized with thiolated RGD (2 mM) and with 0, 0.5, or 2 mM thiolated DWIVA and added to cylindrical molds to form 3D cell-laden Nor-Tet hydrogels (Figure 4A). MSCs encapsulated in 0 mM DWIVA hydrogels and cultured in Osteogenic Medium show significantly more positive staining for ALP (dark blue) than those cultured in Growth Medium (Figure 4B). MSCs cultured in Growth Medium and encapsulated in DWIVA-functionalized HA Nor-Tet hydrogels show an increase in ALP signal with increasing

DWIVA concentration (Figure 4C). A k-means clustering algorithm was applied for MSCs in 3D hydrogels in Growth Medium (negative group) and OS Medium (positive group) to determine a threshold MFI of 48, which covers 95% of ALP(−) MSCs (Figure 4D). The percentage of ALP(+) MSCs in 3D Nor-Tet hydrogels is 19.7% \pm 3.5% (Growth Medium), 20.4% \pm 5.5% (0.50 mM DWIVA), 56.1% \pm 4.6% (2.0 mM DWIVA), and 64.7% \pm 4.3% (OS Medium) (Figure 4E). Confocal images of MSCs cultured in Growth Medium and encapsulated in Nor-Tet hydrogels without (0 mM) or with (2 mM) DWIVA tethering show observable differences in ALP fluorescence (Figure 4F).

To evaluate bone growth *in vivo*, the left and right knee joints of 8-week-old male Lewis rats were opened surgically under sterile conditions. The intercondylar notch of each distal femur was identified, and the intramedullary space of the femur was cleared of native trabecular bone and bone marrow using a 1 mm drill. (Figure 5A). Nor-Tet hydrogel solutions without peptide (Gel group) and with 2.0 mM DWIVA peptide (Peptide group) were injected into the left and right femurs, respectively (Figure 5B). 4 weeks post-injection, rats were euthanized, and femurs were harvested. Microcomputed tomography (micro-CT) was used to image the distal shaft and to create 3D coronal views of the distal shaft and 3D axial views of the distal shaft center (Figure 5C). Increased trabecular bone growth is observed in femurs injected with Peptide-containing Nor-Tet hydrogels when compared to femurs injected with Gel alone, as seen by 3D coronal (Figure 5D) and 3D axial (Figure 5E) views.

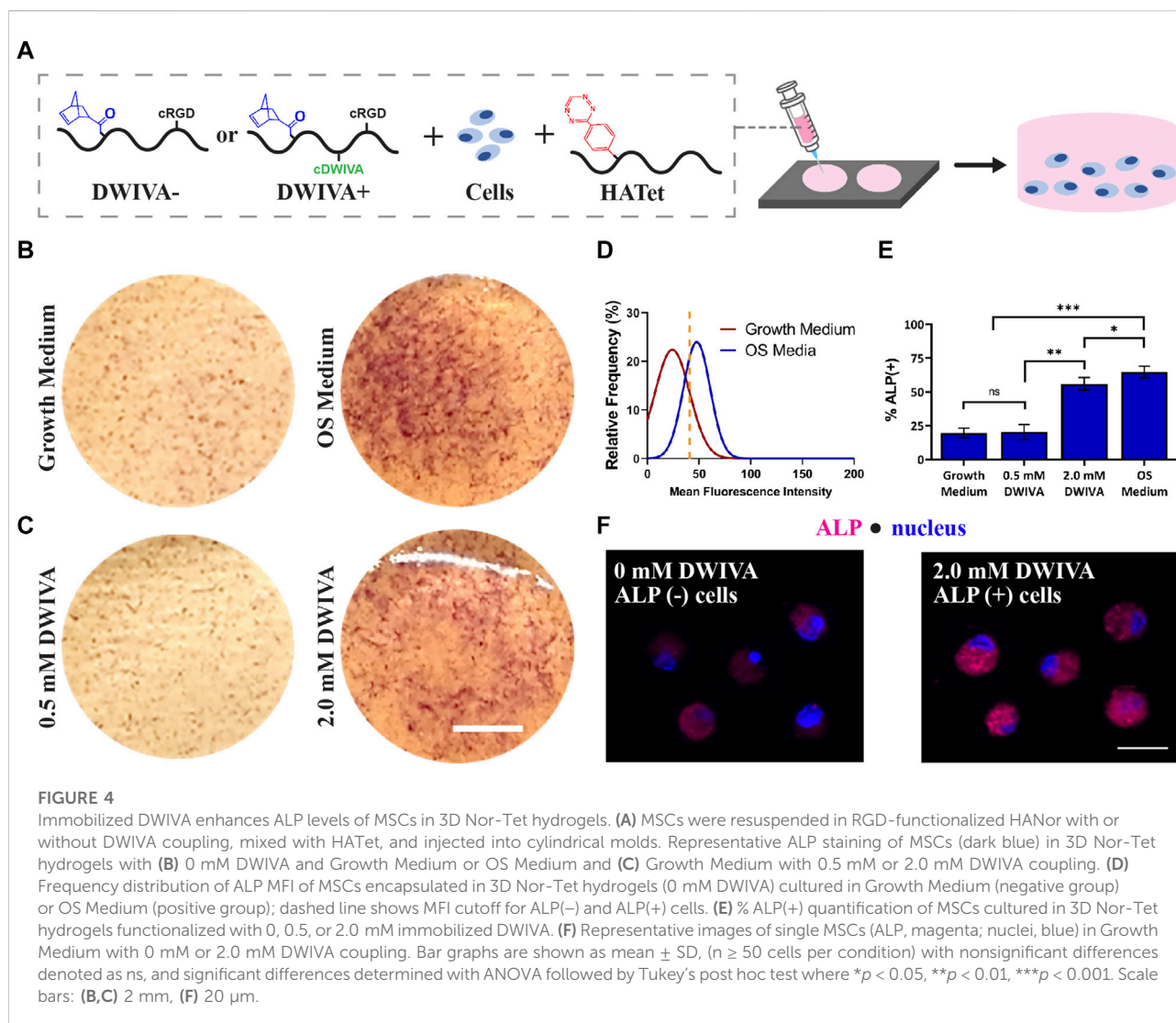




4 Discussion

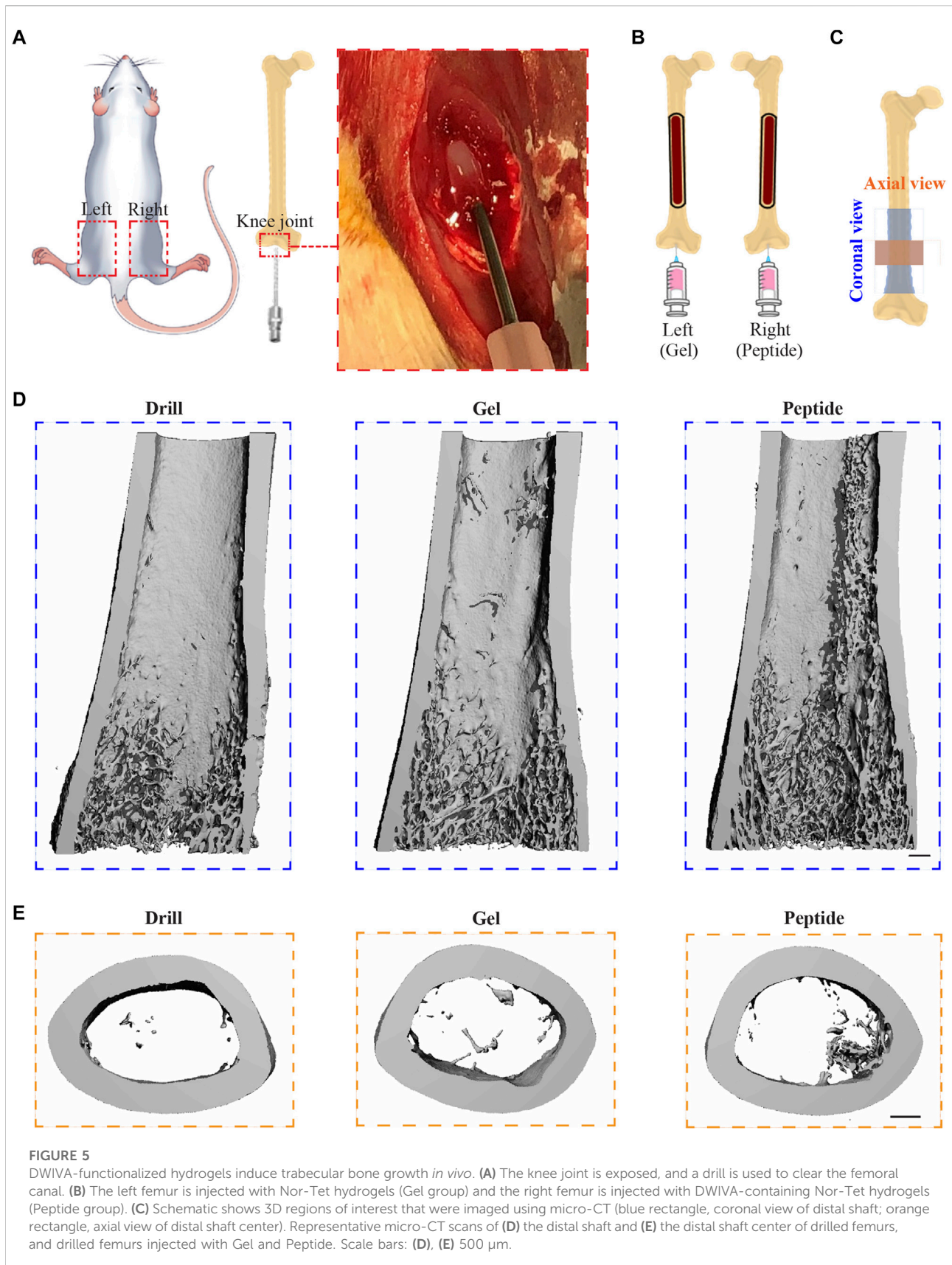
In this study, we developed DWIVA-functionalized self-forming hydrogels that enhance osteogenesis *in vitro* and induce bone growth *in vivo*. While there are other chemistries for forming hydrogels such as photopolymerization and thermogelation, they require some type of catalyst while self-forming hydrogels do not. This method of forming hydrogels makes it suitable for injectability or other applications where catalysts may not be readily available. The hydrogel macromers consist of HA modified with Nor or Tet moieties which upon mixing form covalent networks by undergoing an inverse electron demand Diels-Alder reaction (Supplementary Figure

S3). The 2% w/v macromer formulation used across this entire study allows for sufficient time to extrude the mixed solution without forming inside a syringe or clogging the needle. While this chemistry has been used to develop biocompatible poly(ethylene glycol) (Alge et al., 2013), alginate (Desai et al., 2015), and gelatin (Koshy et al., 2016) self-forming hydrogels, it is challenging to incorporate bioactive motifs into Diels-Alder hydrogels. Here, the carboxyl groups of HA were modified with Nor and Tet, leaving the hydroxyl groups in HA free for additional modifications. This allowed us to pre-functionalize HANor with DWIVA by first modifying hydroxyl groups on HANor with Me moieties, followed by coupling with thiolated DWIVA via a Michael-addition reaction (Figure 1A). Since



DWIVA was coupled to hydroxyl groups, we hypothesized that this should have no impact on Nor-Tet interactions from moieties coupled to carboxyl groups of HA (Figure 1B). To test our hypothesis, we performed rheological tests of 2% w/v HA Nor-Tet hydrogels formed by mixing HATet with HANorMe pre-coupled with different concentrations of DWIVA (0, 0.5, 2.0 mM) (Figures 1C–E). While there was a slight decrease in the storage modulus (G') and gelation time, this was not a significant decrease and may be due to slight variability from time taken to mix and add solutions to the rheometer stage between samples. HA Nor-Tet hydrogels were also pre-formed in cylindrical molds, stored in PBS at 37°C overnight, and compression testing was performed to measure the effects of DWIVA coupling on elastic moduli (E) (Figure 1F). The hydrogels retained their cylindrical geometry at physiological temperature and DWIVA had no effect on stiffness.

DWIVA is the active motif in the wrist epitope of bone morphogenetic protein 2 (BMP-2) (Lee et al., 2009), and growth medium supplemented with BMP-2 causes an osteogenic response on cultured cells (Prall et al., 2013; Samorezov et al., 2016). Soluble BMP-2 has been incorporated with implantable biomaterial scaffolds for bone regeneration (Shields et al., 2006; Garrison et al., 2007; Wong et al., 2008). However, due to diffusion of untethered BMP-2 and its short half-life, high doses of the growth factor were required and serious complications including ectopic bone formation were observed (Shields et al., 2006; Garrison et al., 2007; Wong et al., 2008). Efforts to tether growth factors are limited by low conjugation efficiency and are costly (Madl et al., 2014). Alternatively, short chain mimics of BMP-2 such as DWIVA are inexpensive to synthesize and can be tethered easily. To evaluate the osteogenic properties of DWIVA, MSCs were seeded on glass and cultured



in Growth Medium supplemented with low (0.5 mM) or high (2.0 mM) concentrations of soluble DWIVA. After 7 days in culture, MSCs were stained for ALP, a well-established biomarker of osteogenesis (Lee et al., 2009; Madl et al., 2014). MSCs cultured in Growth Medium and in OS Medium served as control groups and had the lowest and highest observable amount of ALP, respectively (Figures 2A,B). To quantify percentage of ALP(+) MSCs, a mean fluorescence intensity (MFI) histogram of cytoplasmic ALP from MSCs cultured in Growth Medium (negative control) and OS Medium (positive control) was used to identify a cutoff MFI value for ALP(+) cells (Figure 2C). The threshold MFI was set such that 95% of MFI values for MSCs in the ALP(-) group (Growth Medium) were classified as ALP(-). This technique is an adaptation of a k-means clustering-based approach to assign cells to a subpopulation based on specific metrics (Vega et al., 2012), and it minimizes bias for identifying ALP(+) MSCs. Using this approach for MSCs on glass, the threshold MFI was determined to be 52. The Growth Medium and OS Medium ALP MFI histograms had very little overlap and had peak values of 18 and 102, respectively (Figure 2C). Although glass is extremely stiff and rigid substrates favor osteogenic differentiation (Engler et al., 2006), synergy between high mechanics and soluble DWIVA was only observed at high (2.0 mM) DWIVA concentrations. There was no significant difference in ALP(+) MSCs between Growth Medium and low (0.5 mM) DWIVA concentration, while 67% of MSCs were ALP(+) in the high DWIVA concentration group (Figure 2E).

After demonstrating that soluble DWIVA induces increased ALP, we evaluated the osteogenic effects of immobilized DWIVA. Here, HANorMe was first pre-coupled with 2 mM thiolated RGD and different concentrations of thiolated DWIVA (0, 0.5, 2.0 mM). To form peptide-functionalized HA Nor-Tet hydrogels, bioactive HANor was mixed with HATet and the solution polymerized on cylindrical molds, and MSCs were seeded on top (Figure 3A). Since MSCs do not readily adhere to HA, all groups included 2.0 mM RGD, a peptide motif of adhesive fibronectin (Massia and Hubbell, 1990). MSCs attached on all groups, and after 7 days increased intracellular ALP levels were observed with increasing DWIVA concentration (Figure 3B). To minimize bias while identifying ALP(+) MSCs, MFI histograms of MSCs on HA Nor-Tet hydrogels cultured in Growth Medium (negative group) and OS Medium (positive group) were used to identify a threshold MFI (Figure 3C). Through k-means clustering, the cutoff MFI for ALP(+) MSCs was determined to be 50, which is slightly lower than the threshold for the glass group (MFI ≥ 52). There was also significantly more overlap between MFI values for the negative and positive groups, and the MFI peak for the OS Medium group decreased from 102 to 76 (Figure 3C). The decrease in MFI for the positive group could be attributed to the mechanical properties of the HA Nor-Tet hydrogels. At a total macromer concentration of 2% w/v, HA Nor-Tet hydrogels were about 5 kPa, and this low

stiffness does not favor osteogenesis (Engler et al., 2006). Despite being on soft hydrogels, almost 50% of MSCs on Nor-Tet hydrogels with a high concentration (2.0 mM) of immobilized DWIVA were ALP(+) (Figure 3D). Future studies that evaluate the synergistic effects of higher mechanics and immobilized DWIVA on osteogenic differentiation may show increased ALP(+) cells at lower DWIVA concentrations.

To investigate the osteogenic effects of immobilized DWIVA in 3D environments, MSCs were suspended in pre-hydrogel solution consisting of HATet and HANor pre-functionalized with thiolated RGD and different concentrations of thiolated DWIVA (0, 0.5, 2.0 mM) and extruded into molds (Figure 4A). Gross images of 0 mM DWIVA hydrogels stained for ALP show low and high levels of ALP expression of samples cultured in Growth Medium and Osteogenic Medium, respectively (Figure 4B). These control groups confirm that encapsulated MSCs can express ALP in the presence of osteogenic growth factors. A qualitative observation between gross images of hydrogels cultured in Growth Medium with low (0.5 mM) and high (2.0 mM) DWIVA coupling display increased ALP staining with increasing DWIVA concentration (Figure 4C). MSCs are not only highly viable in HA Nor-Tet hydrogels post-extrusion (Supplementary Figure S4), but also respond to immobilized DWIVA in 3D self-forming hydrogels. Using the same k-means clustering approach for the 2D studies, the threshold MFI was determined to be 48, which is slightly lower than the glass (MFI ≥ 52) and 2D hydrogel (MFI ≥ 50) groups. Significant overlap between the negative (Growth Medium) and positive (OS Medium) relative frequency curves was also observed (Figure 4D). Although percentage of ALP(+) MSCs increased with increasing DWIVA concentration, only about 50% of MSCs were classified as ALP(+), even for the OS Medium group (Figure 4E). MSCs encapsulated in the HA Nor-Tet hydrogels remain spherical (Figure 4F), while degradation-mediated cellular traction is necessary for cellular spreading and osteogenesis in 3D hydrogels (Khetan et al., 2013). MSCs encapsulated in DWIVA hydrogels amenable to cell remodeling may be more osteoinductive than those in restrictive hydrogels like the HA Nor-Tet hydrogels used in this study. For example, MSCs in 3D gelatin-based Nor-Tet hydrogels are able to remodel the surrounding hydrogel (Koshy et al., 2016), and replacing the HA backbone of HANorDWIVA with gelatin would allow for 3D cell spreading and DWIVA signaling.

After validating the osteogenic properties of DWIVA-functionalized HA Nor-Tet hydrogels *in vitro*, we were interested in evaluating the ability to grow bone tissue in regions prone to osteoporotic fragility fractures. Specifically, femur fractures can lead to a total hip replacement, and forming nascent trabecular bone in the femur would help prevent fractures from occurring in the first place. To examine the effectiveness of HA Nor-Tet hydrogels in locally regenerating bone *in vivo*, DWIVA-coupled self-forming hydrogels (2 mM) were injected into hollow rat femurs (Figures 5A,B). A high DWIVA concentration was chosen since the percentage of ALP(+) MSCs was highest at 2.0 mM DWIVA. MSCs in HA Nor-Tet hydrogels without DWIVA

functionalization expressed minimal ALP levels and this formulation was injected in contralateral femurs and served as a negative control group. 4 weeks post-injection, the femurs were harvested and micro-CT imaging was utilized to examine the differences in new trabecular bone growth in femurs that were kept hollow (Drill) or injected with uncoupled (Gel) or DWIVA-coupled (Peptide) self-forming hydrogels. 3D coronal views of the distal shaft for the Drill and Gel groups show minimal trabecular bone along the shaft with trabeculae in the metaphysis (bottom), whereas in the Peptide group significant trabecular bone growth is observed along the shaft (Figure 5D). 3D axial views of the distal shaft center reveal almost no trabecular bone in the Drill group, with increasing trabeculae seen in the Gel and Peptide groups (Figure 5E). Since the Gel and Peptide groups were acellular, bone regeneration in the trabecular space would have had to be produced by native cells that migrated into the hydrogel. The migration of native cells into the trabecular space may have been aided by the presence of hyaluronidase, an enzyme that breaks down hyaluronic acid by cleaving its glycosidic bonds, in the femoral shaft (Zhong et al., 1994). Although DWIVA-functionalized hydrogels were exposed to hyaluronidase *in vivo*, the bioactivity of the hydrogel was preserved as shown by improved trabecular bone growth in the Peptide group. Additionally, since hyaluronidase cleaves the glycosidic bonds in the hyaluronic chain, exposure to the enzyme should not interfere with DWIVA conjugation. Enzymatic degradation of HA hydrogels *in vivo* could be replicated *in vitro* by adding exogenous hyaluronidase. By doing so, we will be able to compare the degradation rate of the hydrogel with the rate of trabecular bone formation.

Together, these findings show that injectable, DWIVA-functionalized hydrogels can locally regenerate bone *in vivo* and present opportunities for follow-up studies. Bone regeneration after a fracture can take 6–12 weeks (Yingjie et al., 2007), and the osteogenic effects of DWIVA at later time-points has not been determined. Furthermore, the bioavailability of DWIVA in soluble and tethered form has not been evaluated and it is an area that warrants further study. While we showed that the high (2.0 mM) DWIVA peptide concentration group displayed osteogenic properties *in vitro* and *in vivo*, the peptide coupling chemistry presented here can be used to evaluate the osteoinductive properties of DWIVA at higher peptide concentrations. The HA Nor-Tet hydrogels are amenable to 2D and 3D MSC culture, and the inclusion of DWIVA has an osteogenic effect on resident MSCs. Thus, it would be interesting to evaluate the synergistic effects of MSCs and DWIVA in regenerating bone *in vivo*. Besides the DWIVA wrist epitope of BMP-2, BMP-2 also has a knuckle epitope with the active sequence KIPKASSVPTELSAISTLYLG (KIPKA) (Lee et al., 2009; Madl et al., 2014). The KIPKA sequence is believed to bind to BMP receptor II. Since both receptors I and II are involved in the signaling cascade for BMP-2, it would be beneficial to explore the independent effect of KIPKA and the synergistic effects of KIPKA and DWIVA sequences in locally regenerating bone.

5 Conclusion

We developed an injectable hydrogel with DWIVA, an immobilized mimetic peptide of BMP-2, and demonstrated that it that can regenerate trabecular bone in femurs. We first showed that the effective concentration of DWIVA peptide in self-forming hydrogels can be controlled by changing the amount of peptide added during coupling with HANorMe macromers. We also confirmed that the bioactivity of the DWIVA peptide is preserved post-coupling by showing that ALP expression is enhanced in human MSCs seeded atop (2D) or within (3D) DWIVA-functionalized HA Nor-Tet hydrogels. This hydrogel system has the potential to be used as a targeted therapeutic to improve bone density locally, which is imperative in reducing the incidence of osteoporotic fragility fractures.

Data availability statement

The raw data supporting the conclusion of this article will be made available by the authors, without undue reservation.

Ethics statement

The animal study was reviewed and approved by the Institutional Animal Care and Use Committee (IACUC) at Cooper University Health Care.

Author contributions

KG, TK, and SV conceptualized and designed the research. KG, RG, KD, TK, and SV designed experiments and performed analysis. KG and KD prepared hydrogel samples for *in vivo* studies, KM, VR, EK, PG, and TK performed the animal surgeries, and KG imaged femur explants using a micro-CT scanner. KG, TK, and SV interpreted the data and wrote the manuscript. All authors contributed to the article and approved the submitted version.

Funding

This work was supported by grants from the National Institutes of Health (R21DC018818) and the Camden Health Research Initiative.

Acknowledgments

The authors acknowledge the Penn Center for Musculoskeletal Disorders (PCMD) for providing access to the micro-CT instrument (NIH/NIAMS P30 AR069619). The authors would also like to thank

Sherry Liu, Ph.D. and Yilu Zhou, Ph.D. from the PCMD MicroCT Imaging Core for their technical support. The authors would also like to thank Drew DeLong, V. M. D., M. S. from the Cooper University Health Care Animal Research Program for his expertise in animal care, surgical assistance, and facilitating the ordering and housing of the animals used in this project. The study team would also like to thank Adel Mahjoub, M.D. for his assistance with the surgeries.

Conflict of interest

The authors declare that the research was conducted in the absence of any commercial or financial relationships that could be construed as a potential conflict of interest.

References

- Alge, D. L., Azagarsamy, M. A., Donohue, D. F., and Anseth, K. S. (2013). Synthetically tractable click hydrogels for three-dimensional cell culture formed using tetrazine-norbornene chemistry. *Biomacromolecules* 14, 949–953. doi:10.1021/bm4000508
- Burdick, J. A., and Prestwich, G. D. (2011). Hyaluronic acid hydrogels for biomedical applications. *Adv. Mater.* 23, 41–56. doi:10.1002/adma.201003963
- Cooper, C. (1999). Epidemiology of osteoporosis. *Osteoporos. Int.* 9, S2–S8. doi:10.1007/PL00004156
- Corral, D. A., Amling, M., Priemel, M., Loyer, E., Fuchs, S., Ducy, P., et al. (1998). Dissociation between bone resorption and bone formation in osteopenic transgenic mice. *Proc. Natl. Acad. Sci. U. S. A.* 95, 13835–13840. doi:10.1073/pnas.95.23.13835
- Deligianni, D. D., Missirlis, Y. F., Tanner, K. E., and Bonfield, W. (1991). Mechanical behaviour of trabecular bone of the human femoral head in females. *J. Mater. Sci. Mater. Med.* 2, 168–175. doi:10.1007/BF00692976
- Desai, R. M., Koshy, S. T., Hilderbrand, S. A., Mooney, D. J., and Joshi, N. S. (2015). Versatile click alginate hydrogels crosslinked via tetrazine–norbornene chemistry. *Biomaterials* 50, 30–37. doi:10.1016/j.biomaterials.2015.01.048
- Engler, A. J., Sen, S., Sweeney, H. L., and Discher, D. E. (2006). Matrix elasticity directs stem cell lineage specification. *Cell* 126, 677–689. doi:10.1016/j.cell.2006.06.044
- Garrison, K. R., Donell, S., Ryder, J., Shemilt, I., Mugford, M., Harvey, I., et al. (2007). Clinical effectiveness and cost-effectiveness of bone morphogenetic proteins in the non-healing of fractures and spinal fusion: a systematic review. *Health Technol. Assess.* 11, 1–150. doi:10.3310/HTA11300
- Higley, C. B., Prestwich, G. D., and Burdick, J. A. (2016). Recent advances in hyaluronic acid hydrogels for biomedical applications. *Curr. Opin. Biotechnol.* 40, 35–40. doi:10.1016/j.copbio.2016.02.008
- Ito, Y., and Miyazono, K. (2003). RUNX transcription factors as key targets of TGF- β superfamily signaling. *Curr. Opin. Genet. Dev.* 13, 43–47. doi:10.1016/S0959-437X(03)00007-8
- Khetan, S., Guvendiren, M., Legant, W. R., Cohen, D. M., Chen, C. S., Burdick, J. A., et al. (2013). Degradation-mediated cellular traction directs stem cell fate in covalently crosslinked three-dimensional hydrogels. *Nat. Mater.* 12, 458–465. doi:10.1038/nmat3586
- Koshy, S. T., Desai, R. M., Joly, P., Li, J., Bagrodia, R. K., Lewin, S. A., et al. (2016). Click-crosslinked injectable gelatin hydrogels. *Adv. Healthc. Mater.* 5, 541–547. doi:10.1002/adhm.201500757
- Kwong, F. N. K., Hoyland, J. A., Freemont, A. J., and Evans, C. H. (2009). Altered relative expression of BMPs and BMP inhibitors in cartilaginous areas of human fractures progressing towards nonunion. *J. Orthop. Res.* 27, 752–757. doi:10.1002/jor.20794
- Lee, J.-Y., Choo, J.-E., Choi, Y.-S., Suh, J.-S., Lee, S.-J., Chung, C.-P., et al. (2009). Osteoblastic differentiation of human bone marrow stromal cells in self-assembled BMP-2 receptor-binding peptide-amphiphiles. *Biomaterials* 30, 3532–3541. doi:10.1016/j.biomaterials.2009.03.018
- Li, B., and Aspden, R. M. (1997). Composition and mechanical properties of cancellous bone from the femoral head of patients with osteoporosis or osteoarthritis. *J. Bone Min. Res.* 12, 641–651. doi:10.1359/jbmr.1997.12.4.641
- Li, G.-Z., Randev, R. K., Soeriyadi, A. H., Rees, G., Boyer, C., Tong, Z., et al. (2010). Investigation into thiol-(meth)acrylate Michael addition reactions using amine and phosphine catalysts. *Polym. Chem.* 1, 1196. doi:10.1039/c0py00100g
- Madl, C. M., Mehta, M., Duda, G. N., Heilshorn, S. C., and Mooney, D. J. (2014). Presentation of BMP-2 mimicking peptides in 3D hydrogels directs cell fate commitment in osteoblasts and mesenchymal stem cells. *Biomacromolecules* 15, 445–455. doi:10.1021/bm401726u
- Massia, S. P., and Hubbell, J. A. (1990). Covalent surface immobilization of Arg-Gly-Asp- and Tyr-Ile-Gly-Ser-Arg-containing peptides to obtain well-defined cell-adhesive substrates. *Anal. Biochem.* 187, 292–301. doi:10.1016/0003-2697(90)90459-M
- Mehta, M., Schmidt-Bleek, K., Duda, G. N., and Mooney, D. J. (2012). Biomaterial delivery of morphogens to mimic the natural healing cascade in bone. *Adv. Drug Deliv. Rev.* 64, 1257–1276. doi:10.1016/j.addr.2012.05.006
- Miao, W.-K., Yi, A., Yan, Y.-K., Ren, L.-J., Chen, D., Wang, C.-H., et al. (2015). A poly(polyoxometalate)-b-poly(hexanoic acid) block copolymer: Synthesis, self-assembled micelles and catalytic activity. *Polym. Chem.* 6, 7418–7426. Available at: www.rsc.org/polymers. (Accessed December 4, 2021). doi:10.1039/c5py00855g
- Murakami, N., Saito, N., Takahashi, J., Ota, H., Horiuchi, H., Nawata, M., et al. (2003). Repair of a proximal femoral bone defect in dogs using a porous surfaced prosthesis in combination with recombinant BMP-2 and a synthetic polymer carrier. *Biomaterials* 24, 2153–2159. doi:10.1016/S0142-9612(03)00041-3
- Osterhoff, G., Morgan, E. F., Shefelbine, S. J., Karim, L., McNamara, L. M., Augat, P., et al. (2016). Bone mechanical properties and changes with osteoporosis. *Injury* 47, S11–S20. doi:10.1016/S0020-1383(16)47003-8
- Park, J. S., Yang, H. N., Jeon, S. Y., Woo, D. G., Na, K., Park, K.-H., et al. (2010). Osteogenic differentiation of human mesenchymal stem cells using RGD-modified BMP-2 coated microspheres. *Biomaterials* 31, 6239–6248. doi:10.1016/j.biomaterials.2010.05.002
- Prall, W. C., Haasters, F., Heggebö, J., Polzer, H., Schwarz, C., Gassner, C., et al. (2013). Mesenchymal stem cells from osteoporotic patients feature impaired signal transduction but sustained osteoinduction in response to BMP-2 stimulation. *Biochem. Biophys. Res. Commun.* 440, 617–622. doi:10.1016/j.bbrc.2013.09.114
- Rachner, T. D., Khosla, S., and Hofbauer, L. C. (2011). Osteoporosis: Now and the future. *Lancet* 377, 1276–1287. doi:10.1016/S0140-6736(10)62349-5
- Samorezov, J. E., Headley, E. B., Everett, C. R., and Alsberg, E. (2016). Sustained presentation of BMP-2 enhances osteogenic differentiation of human adipose-derived stem cells in gelatin hydrogels. *J. Biomed. Mater. Res. A* 104, 1387–1397. doi:10.1002/jbm.a.35668
- Seol, Y.-J., Park, Y.-J., Lee, S.-C., Kim, K.-H., Lee, J.-Y., Kim, T.-I., et al. (2006). Enhanced osteogenic promotion around dental implants with synthetic binding motif mimicking bone morphogenetic protein (BMP)-2. *J. Biomed. Mater. Res. A* 77A, 599–607. doi:10.1002/jbm.a.30639

Publisher's note

All claims expressed in this article are solely those of the authors and do not necessarily represent those of their affiliated organizations, or those of the publisher, the editors and the reviewers. Any product that may be evaluated in this article, or claim that may be made by its manufacturer, is not guaranteed or endorsed by the publisher.

Supplementary material

The Supplementary Material for this article can be found online at: <https://www.frontiersin.org/articles/10.3389/fbiom.2022.948493/full#supplementary-material>

- Shields, L. B. E., Raque, G. H., Glassman, S. D., Campbell, M., Vitaz, T., Harpring, J., et al. (2006). Adverse effects associated with high-dose recombinant human bone morphogenetic protein-2 Use in anterior cervical spine fusion. *Spine* 31, 542–547. doi:10.1097/01.brs.0000201424.27509.72
- Smeds, K. A., and Grinstaff, M. W. (2000). Photocrosslinkable polysaccharides for *in situ* hydrogel formation. *J. Biomed. Mater. Res.* 54 (1), 115–121. doi:10.1002/1097-4636(200101)54:1<115:aid-jbm14>3.0.co;2-q
- Sozen, T., Ozisik, L., and Calik Basaran, N. (2017). An overview and management of osteoporosis. *Eur. J. Rheumatol.* 4, 46–56. doi:10.5152/eurjrheum.2016.048
- Takahashi, Y., Yamamoto, M., and Tabata, Y. (2005). Enhanced osteoinduction by controlled release of bone morphogenetic protein-2 from biodegradable sponge composed of gelatin and β -tricalcium phosphate. *Biomaterials* 26, 4856–4865. doi:10.1016/j.biomaterials.2005.01.012
- Toole, B. P. (2001). Hyaluronan in morphogenesis. *Seminars Cell Dev. Biol.* 12, 79–87. doi:10.1006/scdb.2000.0244
- Toole, B. P. (2004). Hyaluronan: from extracellular glue to pericellular cue. *Nat. Rev. Cancer* 4, 528–539. doi:10.1038/nrc1391
- Tsuji, K., Bandyopadhyay, A., Harfe, B. D., Cox, K., Kakar, S., Gerstenfeld, L., et al. (2006). BMP2 activity, although dispensable for bone formation, is required for the initiation of fracture healing. *Nat. Genet.* 38, 1424–1429. doi:10.1038/ng1916
- Tu, K. N., Lie, J. D., Wan, C. K. V., Cameron, M., Austel, A. G., Nguyen, J. K., et al. (2018). Osteoporosis: A review of treatment options. *PT* 43, 92–104. Available at: <https://www.ncbi.nlm.nih.gov/pmc/articles/PMC5768298> (Accessed March 21, 2022).
- Van der Voort, D. J. M., Geusens, P. P., and Dinant, G. J. (2001). Risk factors for osteoporosis related to their outcome: Fractures. *Osteoporos. Int.* 12, 630–638. doi:10.1007/S001980170062
- Vega, S. L., Liu, E., Patel, P. J., Kulesa, A. B., Carlson, A. L., Ma, Y., et al. (2012). High-content imaging-based screening of microenvironment-induced changes to stem cells. *SLAS Discov.* 17, 1151–1162. doi:10.1177/1087057112453853
- Vega, S. L., Kwon, M. Y., Song, K. H., Wang, C., Mauck, R. L., Han, L., et al. (2018). Combinatorial hydrogels with biochemical gradients for screening 3D cellular microenvironments. *Nat. Commun.* 9, 614. doi:10.1038/s41467-018-03021-5
- Waite, K. A., and Eng, C. (2003). From developmental disorder to heritable cancer: it's all in the BMP/TGF- β family. *Nat. Rev. Genet.* 4, 763–773. doi:10.1038/nrg1178
- Wong, D. A., Kumar, A., Jatana, S., Ghiselli, G., and Wong, K. (2008). Neurologic impairment from ectopic bone in the lumbar canal: a potential complication of off-label PLIF/TLIF use of bone morphogenetic protein-2 (BMP-2). *Spine J.* 8, 1011–1018. doi:10.1016/j.spinee.2007.06.014
- Wrana, J. L. (2000). Regulation of Smad activity. *Cell* 100, 189–192. doi:10.1016/S0092-8674(00)81556-1
- Wright, N. C., Looker, A. C., Saag, K. G., Curtis, J. R., Delzell, E. S., Randall, S., et al. (2014). The recent prevalence of osteoporosis and low bone mass in the United States based on bone mineral density at the femoral neck or lumbar spine. *J. Bone Min. Res.* 29, 2520–2526. doi:10.1002/jbmr.2269
- Yingjie, H., Ge, Z., Yisheng, W., Ling, Q., Hung, W. Y., Kwoksui, L., et al. (2007). Changes of microstructure and mineralized tissue in the middle and late phase of osteoporotic fracture healing in rats. *Bone* 41, 631–638. doi:10.1016/j.bone.2007.06.006
- Yousefi, F., Kandel, S., and Pleshko, N. (2018). Infrared spectroscopic quantification of methacrylation of hyaluronic acid: A scaffold for tissue engineering applications. *Appl. Spectrosc.* 72, 1455–1466. doi:10.1177/0003702818785353
- Zebaze, R. M., Ghasem-Zadeh, A., Bohte, A., Iuliano-Burns, S., Mirams, M., Price, R. I., et al. (2010). Intracortical remodelling and porosity in the distal radius and post-mortem femurs of women: a cross-sectional study. *Lancet* 375, 1729–1736. doi:10.1016/S0140-6736(10)60320-0
- Zhao, B., Katagiri, T., Toyoda, H., Takada, T., Yanai, T., Fukuda, T., et al. (2006). Heparin potentiates the *in vivo* ectopic bone formation induced by bone morphogenetic protein-2. *J. Biol. Chem.* 281, 23246–23253. doi:10.1074/jbc.M511039200
- Zhong, S. P., Campoccia, D., Doherty, P. J., Williams, R. L., Benedetti, L., Williams, D. F., et al. (1994). Biodegradation of hyaluronic acid derivatives by hyaluronidase. *Biomaterials* 15, 359–365. doi:10.1016/0142-9612(94)90248-8